Oleic acid-induced steatosis model establishment in LMH cells and its effect on lipid metabolism

Huiqi Song,[*,‡,§] Ruizhi Yang,[*,‡,§] Jiahao Zhang,[†,‡,§] Pengliang Sun,[†,‡,§] Xiaoyue Xing,[†,‡,§] Lan Wang,[†,‡,§] Ta Sairijima,[†,‡,§] Yahui Hu,[†,‡,§] Yang Liu,[†,‡,§] Huixu Cheng,[†,‡,§] Qiulin Zhang,[†,‡,§] and Lianrui Li [*,†,‡,§,1]

[*]*College of life science and technology, Tarim University, Alar 843300, Xinjiang, China;* [†]*College of animal science and technology, Alar 843300, Xinjiang, China;* [‡]*Key Laboratory of Tarim Animal Husbandry Science and Technology, Xinjiang Production and Construction Corps, Alar 843300, Xinjiang ,China; and* [§]*Engineering Laboratory of Tarim Animal Diseases Diagnosis and Control, Xinjiang Production and Construction Corps, Alar 843300, Xinjiang, China*

ABSTRACT Hepatic steatosis is a highly prevalent liver disease, yet research on it is hampered by the lack of tractable cellular models in poultry. To examine the possibility of using organoids to model steatosis and detect it efficiently in leghorn male hepatocellular (**LMH**) cells, we first established steatosis using different concentrations of oleic acid (**OA**) (0.05 −0.75 mmol/L) for 12 or 24 h. The subsequent detections found that the treatment of LMH cells with OA resulted in a dramatic increase in intracellular triglyceride (**TG**) concentrations, which was positively associated with the concentration of the inducing OA (R^2 > 0.9). Then, the modeled steatosis was detected by flow cytometry after NileRed staining and it was found that the intensity of NileRed-A was positively correlated with the TG concentration (R^2 > 0.93), which demonstrates that the flow cytometry is suitable for the detection of steatosis in LMH cells. According to the detection results of the different steatosis models, we confirmed that the optimal induction condition for the establishment of the steatosis model in LMH cells is OA (0.375 mmol/L) incubation for 12 h. Finally, the transcription and protein content of fat metabolism-related genes in steatosis model cells were detected. It was found that OA-induced steatosis could significantly decrease the expression of nuclear receptor PPAR-γ and the synthesis of fatty acids (SREBP-1C, ACC1, FASN), increasing the oxidative decomposition of triglycerides (CPT1A) and the assembly of low-density lipoproteins (MTTP, ApoB). Sterol metabolism in model cells was also significantly enhanced (HMGR, ABCA1, L-BABP). This study established, detected, and analyzed an OA-induced steatosis model in LMH cells, which provides a stable model and detection method for the study of poultry steatosis-related diseases.

Key words: LMH cells, steatosis model, oleic acid, flow cytometry, lipid metabolism

2022 Poultry Science 102:102297
https://doi.org/10.1016/j.psj.2022.102297

INTRODUCTION

Hepatic steatosis broadly represents an excess accumulation of fat (mainly triacylglycerols) in the parenchymal cells (hepatocytes) of the liver, resulting in obviously microscopically visible lipid droplets within the cytoplasm (Matteoni et al., 1999; Marchesini et al., 2001; Browning et al., 2004; Masahide et al., 2005). The accumulation of fat in the hepatocytes is caused by an imbalance between lipid availability (from circulating lipid uptake and/or de novo lipogenesis [**DNL**]) and lipid disposal (via fatty acid oxidation and/or triacylglycerol-rich lipoprotein secretion) in the liver (Neuschwander-Tetri, 2001). Occasional triacylglycerol droplets in hepatocytes are considered normal, but when more than 5% of hepatocytes contain lipid droplets, a histopathological diagnosis of hepatic steatosis is established.

Hepatic steatosis is an initial manifestation of severely progressive liver diseases. Simple steatosis of the liver in chicken may develop into steatohepatitis, liver fibrosis, fatty liver syndrome (**FLS**) (Shini et al., 2020; Tan et al., 2020), and even fatty liver hemorrhagic syndrome (**FLHS**) (Liu et al., 2016; Meng et al., 2021; Tan et al., 2021) if no efficacious intervention is made for the

Received October 23, 2021.
Accepted October 24, 2022.

[1]Corresponding author: lilianrui51@163.com

hepatic steatosis at an early stage. Hepatocellular steatosis in chicken is the consequence of various nutritional factors and associated diseases such as obesity (Liang et al., 2015), body hepatitis (FAdV-4) (Yuan et al., 2021), high endogenous estrogen levels (Haghighi-Rad and Polin, 1981), and other factors.

In many fatty livers studied so far, artificially induced hepatic steatosis models have been used to investigate the molecular mechanisms of dynamic changes, as well as abnormalities, dysfunction, and regulation of lipid metabolism in hepatocytes. Hepatic steatosis models can be largely divided into 2 classes: in vitro and in vivo. In vitro hepatic steatosis models have been established using interventions leveraging dietary modifications to feed target animals, such as high-fat and high-sugar diets, etc. However, those in vivo hepatic steatosis models have disadvantages, such as requiring a long time, individual differences between each model, complex influencing factors in the experiment, etc (Lau et al., 2017; Febbraio et al., 2019). In contrast, because in vitro hepatic steatosis models have the advantage of requiring a relatively shorter time and are easy and stable enough for repetition, they have an extraordinary advantage in laboratory research. Oleic acid (**OA**)-induced steatosis has been studied extensively in the hepatocytes of many mammalian species, such as in HepG2, L02, Chang liver cells, etc (Feldstein et al., 2004; Yan et al., 2015; Hu et al., 2019). However, no steatosis model in hepatocytes from poultry has been studied so far.

In this study, we developed a poultry hepatocyte steatosis model treating leghorn male hepatocellular (**LMH**) cells with OA and determined the optimal treatment conditions for the establishment of the steatosis model. In addition, the study also determined the reliability and accuracy of flow cytometry in detecting hepatocyte steatosis. Finally, we evaluated the effects of OA on fat and cholesterol metabolic pathways in the steatosis model. Overall, the results presented here provide a useful context for steatosis research in hepatocytes from poultry.

MATERIALS AND METHOD

Cell Cultures and Oleic Acid-Induced Steatosis Model Establishment

LMH cells (chicken hepatoma cell line) were cultured in Dulbecco's modified Eagle medium (**DMEM**) (Life Technologies, 11995) supplemented with 100 mg/ml streptomycin, 100 units/ml penicillin, and 10% fetal bovine serum (FBS; Gibco, 10099−141) at 37°C in the presence of 5% CO_2 in an incubator.

Monolayer LMH cells were grown to approximately 85% confluence in six well plates and were incubated with different concentrations of OA (Sodium oleate; Sigma-Aldrich, 143-19-1)-bovine serum albumin (**BSA**) (7.5% BSA solution; Sigma-Aldrich, H1130), (0.05, 0.15, 0.375, 0.75 mmol/L) + BSA (0.5%) or BSA (0.5%), for 12 or 24 h to induce steatosis.

Antibodies and Reagents

Primary antibodies were used: rabbit anti-LXR-α (A5313) purchased from Bimake; Rabbit anti-PPAR-α (ab178865); Mouse anti-SREBP-1C (ab3259); Rabbit anti-FASN (ab230988); Mouse anti-GAPDH (ab8245); and Rabbit anti-MTTP (ab186446). All the above antibodies were obtained from Abcam. Oleic Acid (YZ-111621) and NileRed (G1262) from Solarbio. Fluorescein isothiocyanate (**FITC**)-conjugated secondary antibodies were purchased from Dako. Horseradish peroxidase (HRP)-conjugated secondary antibodies were purchased from Sigma.

SDS-PAGE and Western Blotting

The whole-cell lysates prepared at different time points were treated with RIPA lysis buffer (Beyo time, P0013B) and 1 mmol/L phenylmethane sulfonyl fluoride (PMSF, Beyo time, ST506-2). The total protein concentration was measured by the Bicarboxylic acid protein analysis kit (Thermo Scientific, 23225). The same amount of total protein was analyzed by polyacrylamide gel electrophoresis and then transferred to the nitrocellulose membrane (PAL, 66485). Then, NC membranes were sealed with skim milk at 37°C for 2 h, incubated overnight with different first antibodies at 4°C, and then incubated with second antibodies coupled with horseradish peroxidase at 37°C for 2 h; the second antibody was detected by the SuperSignal West Femto Maximum Sensitivity Substrate (Thermo Scientific, 34096) and then imaged by a chemiluminescence instrument.

Indirect Immunofluorescence and Confocal Microscopy

Briefly, monolayer LMH cells grew to approximately 85% confluence in chamber slides (BD) and induced steatosis by oleic acid; the cells were washed with PSBS and fixed in 4% paraformaldehyde (**PFA**) for 15 min, followed by incubation with 4',6'-diaminido-2-phenylindole (**DAPI**) at a concentration of 1 μg/mL for 5 min at 37°C. The cells were then stained with NileRed at a concentration of 0.1 μg/mL, at 37°C for 20 min. Following further washing with PBS, the slides were dried and mounted with fluorescence mounting media and examined under a Nikon AIR confocal laser microscope system (Nikon Instruments, Inc., Melville, NY).

Flow Cytometry Analysis

LMH cells induced steatosis by oleic acid and were dispersed into single cells by trypsin digestion. The cells were washed with PBS and fixed in 4% paraformaldehyde (PFA) for more than 15 min, then incubated with NileRed at a concentration of 0.1 μg/mL 37°C for 15 min. They were then further washed with PBS more than 3 times. Finally, Flow Cytometry Analyses of steatosis were directly performed on the cells following

isolation. The cells were acquired using the ACEA NovoCyte flow cytometer (ACEA Biosciences) and were analyzed using NovoExpress software v.1.4.0. To ensure stringent single-cell gating, cell debris were excluded using SSC and FSC height and width as recommended by the Flow Cytometry Network. Appropriate isotype controls were used in all steps.

Kit Detection

Trans Detect Cell Counting Kit (**CCK**) from the Trans Gen. Cell triglyceride (**TG**) enzymatic assay kit (E1013) from APPLYGEN was used. All the kits mentioned above were tested in accordance with the technical operation manual of the product.

RNA Preparation and Reverse Transcription-Polymerase Chain Reaction (RT-PCR) Analysis

LMH cells were treated according to different experiments (n = 3), and total cellular RNA was extracted by the RNeasy Mini Kit (Qiagen, 74104) according to the manufacturer's protocol. cDNA was reverse-transcribed with 4 mg of total RNA as the template, which was amplified by following the procedures described in the Trans Script II One-Step gDNA Removal and cDNA Synthesis SuperMix (Trans Gen Biotech, AH311-03). Quantitative real-time polymerase chain reaction was performed with TransStart Tip Green qPCR SuperMix (Trans Gen Biotech, AQ141-04). Analysis of relative gene expression data was done using real-time Quantitative PCR and the $2^{-\Delta\Delta Ct}$ method.

Statistical Analysis

Statistical analysis was performed using GraphPad Prism Software. Data derived from the cell line were presented as mean±SD and assessed by Student's t-test. Each experiment was repeated at least three times and the error bars represent the SD. ($P < 0.05$ *, $P < 0.01$ **, $P < 0.001$ ***, $P < 0.0001$ ****) was considered to be statistically significant.

RESULTS

LMH Induction With OA Markedly Increased the Cellular Triglyceride Level, Which was Positively Associated With the Concentration of the Inducing OA

First, LMH was treated with different concentrations of OA and we detected cellular viability by a CCK assay to ensure that the OA concentrations used did not impact metabolic activity. Statistical analysis revealed that except for the treatment with 0.75 mmol/L OA for 24 h, other concentrations of OA (0.05−0.75 mmol/L) for 12 or 24 h do not impair the proliferation or cytotoxic activity of LMH cells (Figure 1A). The results illustrate that OA is not cytotoxic to cells, at least at the concentration we used, except for the 0.75 mmol/L OA at 24 h. Next, we measured the levels of triglycerides (**TG**s) in the LMH cells. The results showed that there was a significant oleic acid concentration-dependent (0.05−0.75 mmol/L) increase in accumulations of intracellular TG in LMH cells for all OA processing groups, compared with the controls and BSA. In addition, after LMH was treated with OA at the same concentration for two different time points, the concentrations of intracellular TGs in the 12-h treatment group were significantly higher than those in the 24-h treatment group (Figure 1B). We further investigated the relationship between OA and the concentration of intracellular TG by linear regression analysis. The results demonstrate that intracellular triglyceride accumulations and concentration of OA show a highly significant linear relationship, 12 h: $R^2 = 0.9180$ $P < 0.0001$, 24 h: $R^2 = 0.9094$ $P < 0.0001$. This suggested that these findings confirmed that OA could effectively induce steatosis without affecting the activity of LMH cells.

Lipid Droplets in the Hepatocyte Steatosis Model Induced by OA Images Acquired Through Confocal Microscopy

In addition to the significant increase in TG content, the appearance of clearly visible oil droplets in cells is also an important pathological change of hepatocyte steatosis. Therefore, we stained intracellular oil droplets by NileRed to evaluate oleic acid-induced steatosis. Most lipids in the cells are stained light red trace and display a scattered distribution in cells, such as glycolipids and phospholipids, etc. Fat is mainly the form of triglycerides stored as lipid droplets in hepatocytes when steatosis, stained with NileRed, shows bright red dots that vary in size, which depends on the size of the lipid droplets. The LMH cells were stained with NileRed stain and observed with a fluorescence confocal microscope (Figure 2). The IFA results revealed that after OA (0.05−0.75 mmol/L) induction for 12 h, these cells displayed round orange droplets within the cytoplasm upon oil red staining, which indicates the formation of lipid droplets. When the concentration of OA was higher than 0.15 mmol/L, a large number of lipid droplets appeared, and the number and diameter of the droplets increased with increasing concentration of the inducing OA. LMH was treated with the same concentrations of OA for 24 h, and the numbers and diameters of the droplets reduced compared with those for 12 h. This suggests that 12-h incubation is more suitable than 24-h incubation when establishing a model for steatosis in LMH cells using OA.

The Hepatic Steatosis Model was Assessed Using Flow Cytometry

To better understand the alterations of the lipid droplets in the steatosis model, the NileRed stained cells

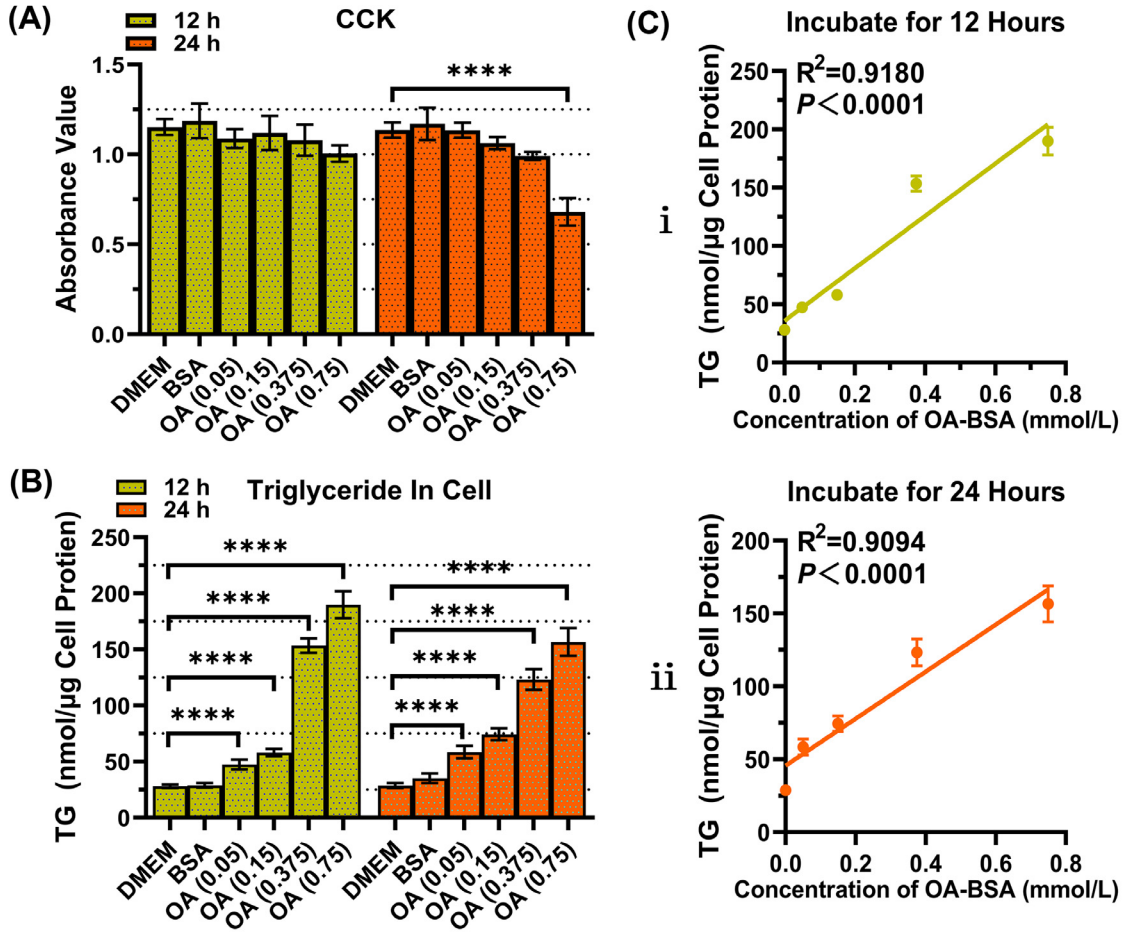

Figure 1. Oleic acid (OA) markedly increased the cellular triglyceride (TG) levels in LMH cells and the concentration of TGs was positively correlated with the concentration of the inducing OA. To determine the maximum concentration of OA, the different concentrations of OA (0.05−0.75 mmol/L) were used to treat LMH for 12/24 h and detect cell activity by CCK respectively (A). We also tested the intracellular triglyceride content in the same model (B). To assess the relationship between the concentration of inducing OA and the concentration of intracellular triglycerides, the concentration of OA was plotted on the x-axis and the concentration of intracellular triglycerides on the y-axis, at 12 and 24 h (C).

were examined using flow cytometry. Cells were first gated based on forwarding (FSC-A) and side (SSC-A) scatters (measuring cell size and granularity, respectively) to exclude debris (Figure 3A). All experimental groups were used to draw gates on the control groups of DMEM at 12 h. Living cells were included in a polygon gate, whereas the remaining cells (mostly debris) were excluded. Cells treated with only DMEM as controls have 97% intact cells, and debris was scarcely detected. When LMH was treated with OA, the cell fragments gradually increased as the concentration of OA increased. When the treatment concentration of OA reached 0.375 mmol/L in 12 h, the cell debris rate reached approximately 26%, and debris progressively increased to 60% when OA reached 0.75 mmol/L. In addition, compared with treatment for 12 h at the same concentration of OA, LMH cells have more cell debris when treated with OA for 24 h.

We next studied Red fluorescence (NileRed-A) and side (SSC-A) scatters, and a DMEM stained with NileRed was referred to as the baseline (Figure 3B). Flow cytometry showed negative staining for NileRed with lower granularity at the lower left quadrant (Q3−3), NileRed negative staining and increased cell granularity in the lower right quadrant, NileRed positive staining and lower cell granularity in the upper right quadrant, and NileRed negative staining and increased granularity within cells in the upper left quadrant; those quadrants were labeled with the percentage of events in each. We observed that there was a significant increase in the fluorescence intensity of NileRed (Q3−2+Q3−4) with a concentration-dependent increased induction. The NileRed (Q3−2+Q3−4) positivity rate increased gradually with the increase in inducing OA concentration, from 7% to 98% at 12h-incubation. The same treatment for 24 h resulted in the NileRed (Q3−2+Q3−4) positivity rate increasing from 1% to 90%. Cellular granularity (side scatter [SSC-A]) data showed that the granularity (Q3−2) within cells increased with an increasing degree of steatosis. LMH cells treated with OA at the same concentrations for 24 h had higher granularity compared with those treated for 12 h.

Integrative Analysis of the Flow Cytometry Data to Identify a new Method for Testing Hepatic Steatosis

To evaluate this novel assay for flow cytometry, the data were analyzed by GraphPad. The results showed

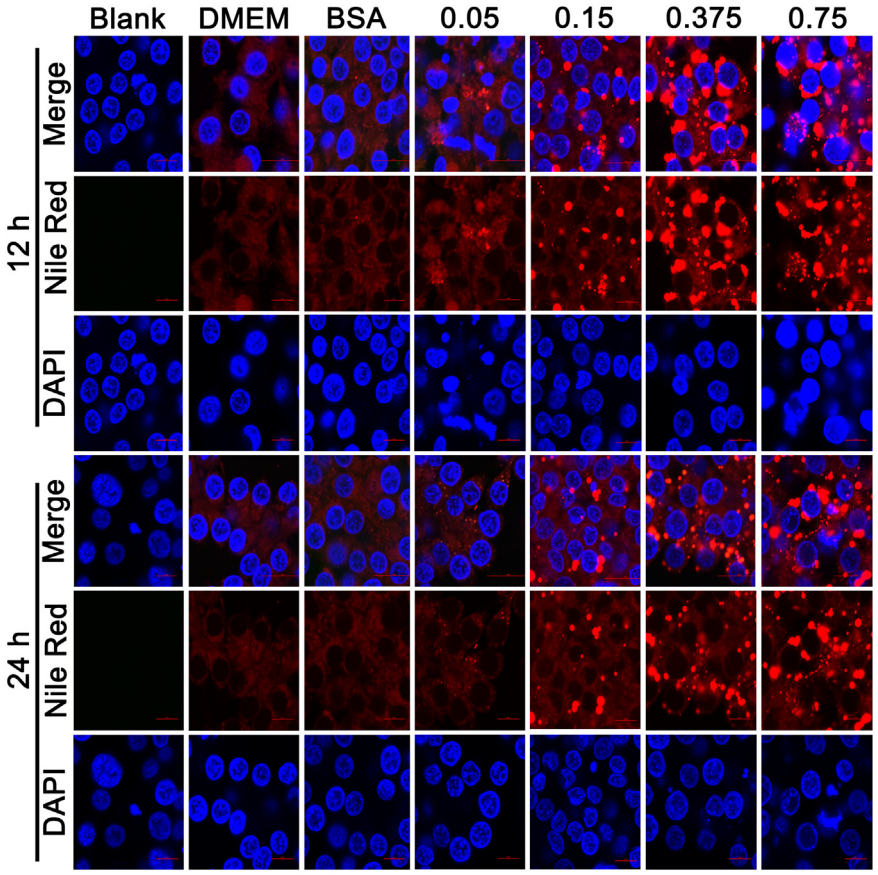

Figure 2. The oil drop in the steatosis model of LMH cells was observed by confocal microscopy. The cells were stained with NileRed (Red) and DAPI (Blue).

that the enhancement of the NileRed fluorescence intensity increased with the increasing inducing concentration of OA or the content of intracellular triglycerides, both for 12 and 24 h (Figure 4A i), which is in agreement with the simulation results shown in Figures 2 and 3. Linear regression analyses were performed between NileRed fluorescence intensity and inducing OA concentrations (Figure 4B i and ii) or the content of intracellular triglycerides (Figure 4C i and ii), which showed a strong positive correlation between them: NileRed fluorescence intensity with inducing OA concentrations (12 h: $R^2 = 0.98$, $P = 0.0012$, 24h: $R^2 = 0.9977$, $P < 0.0001$), NileRed fluorescence intensity with the content of intracellular TGs (12h: $R^2 = 0.9676$, $P < 0.0001$, 24h: $R^2 = 0.9317$, $P < 0.0001$). Additionally, information about the cell size (FSC) showed a small increase in the steatosis model both at 12 and 24 h (Figure 4b i). However, we did not find a clear dependence between cell size (FSC) and inducing OA concentrations (Figure 4B v and vi) or the content of intracellular triglycerides (Figure 4C v and vi) by linear regression analysis, except for the group of 24 h OA-treatment. Finally, increased granularity (SSC-A) within the cells was found in OA-induced steatosis model cells (Figure 4C i), which shows a good linear relationship with the inducing OA concentrations (Figure 4B iii and iv) or the content of intracellular TG (Figure 4c iii and iv), both at 12 and 24 h after treatments. The correlation analysis results of Figures 4B and 4C show a positive correlation between the inducing OA concentrations and SSC-A (12 h: $R^2 = 0.9453$, $P = 0.0055$, 24 h: $R^2 = 0.9900$, $P = 0.0004$) and between the content of intracellular TGs and SSC-A (12 h: $R^2 = 0.9130$, $P < 0.0001$, 24 h: $R^2 = 0.8914$, $P < 0.0001$). The above results indicate that the NileRed fluorescence (NileRed-A) and the cellular granularity (SSC-A) correspond to an increasing concentration of inducing OA or intracellular concentration of TGs, which demonstrated that the flow cytometry analysis of intracellular staining for NileRed gives good indications on the degree of steatosis in LMH cells.

Effect of OA on the Adipose Metabolic Pathway in the Process of Steatosis in LMH Cells

To test the effect of OA on hepatocyte fat metabolism, an analysis of the expression of the protein that regulates hepatic fat metabolism was performed by western blotting. It suggested that several lipid metabolic pathways, including the impairment of lipid synthesis, lipid oxidation, and transport of lipoproteins, are related to the development of hepatic steatosis. Liver X Receptor, peroxisome proliferators-activated receptor-α (**PPAR-α**), and peroxisome proliferators-activated receptor-γ (**PPAR-γ**) are ligand-induced nuclear receptors, which could use intracellular fatty acids and sterols as ligands for metabolic processes.

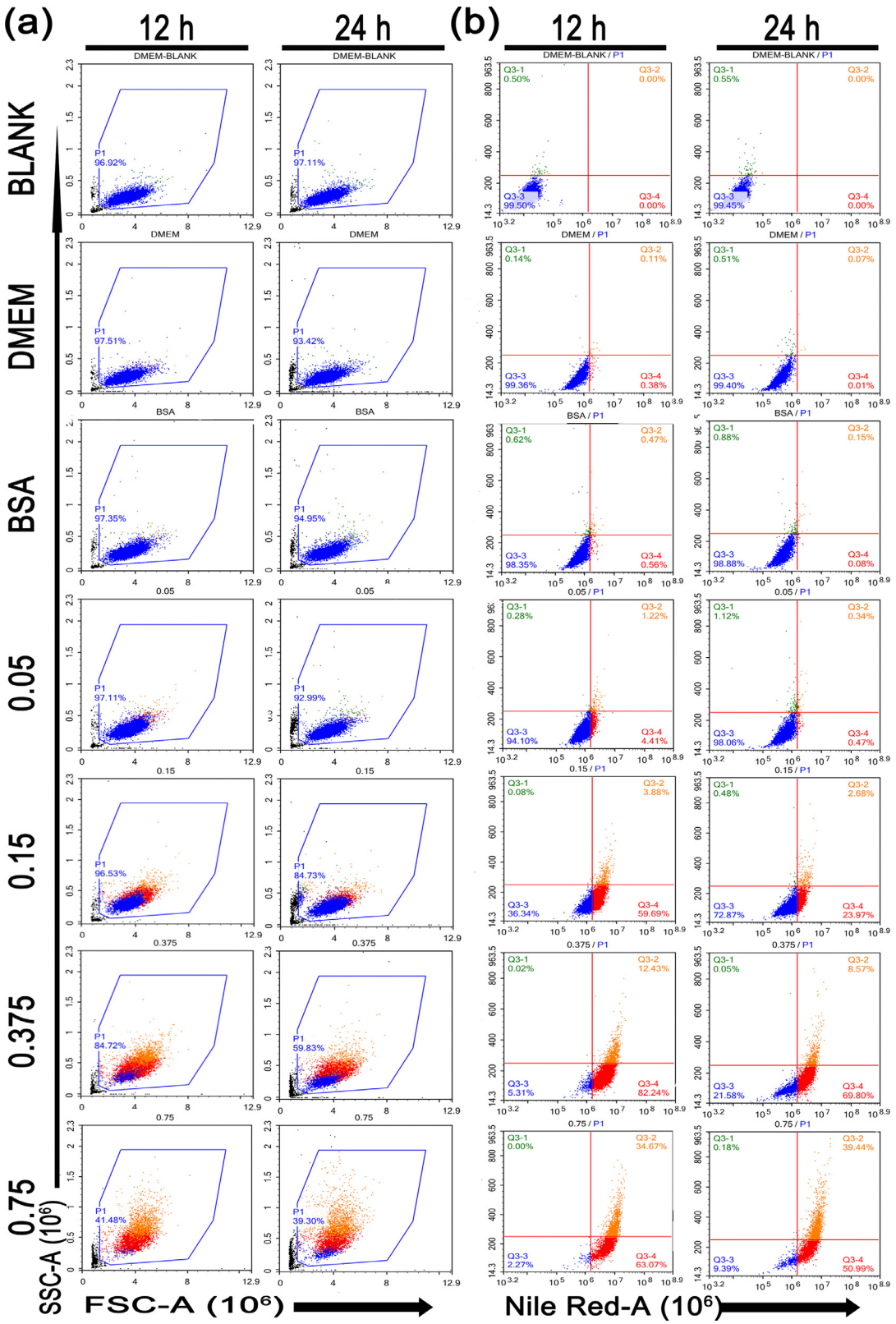

Figure 3. Flow cytometry was used to characterize the OA-BSA-induced steatosis in LMH cells. LMH cells were fixed and treated as described in Figure 2. Then, intracellular NileRed fluorescence intensity was measured by flow cytometry. The representative scatter plots show the forward (FSC-A) and side scatter (SSC-A) distribution of LMH cells at 12 or 24 h (A). The intensity of Red fluorescence (NileRed-A) and side (SSC-A) scatter was measured (B).

The results of western blotting (**WB**) and WB analysis for LXR show that the addition of OA did not affect the expression of LXR proteins (Figure 5A and B). Additionally, the PPAR-γ protein was also significantly reduced by OA compared with the control group but there was no significant concentration dependence. PPAR-α was not significantly affected by OA-BSA incubation, even at 0.75 mmol/L. To further

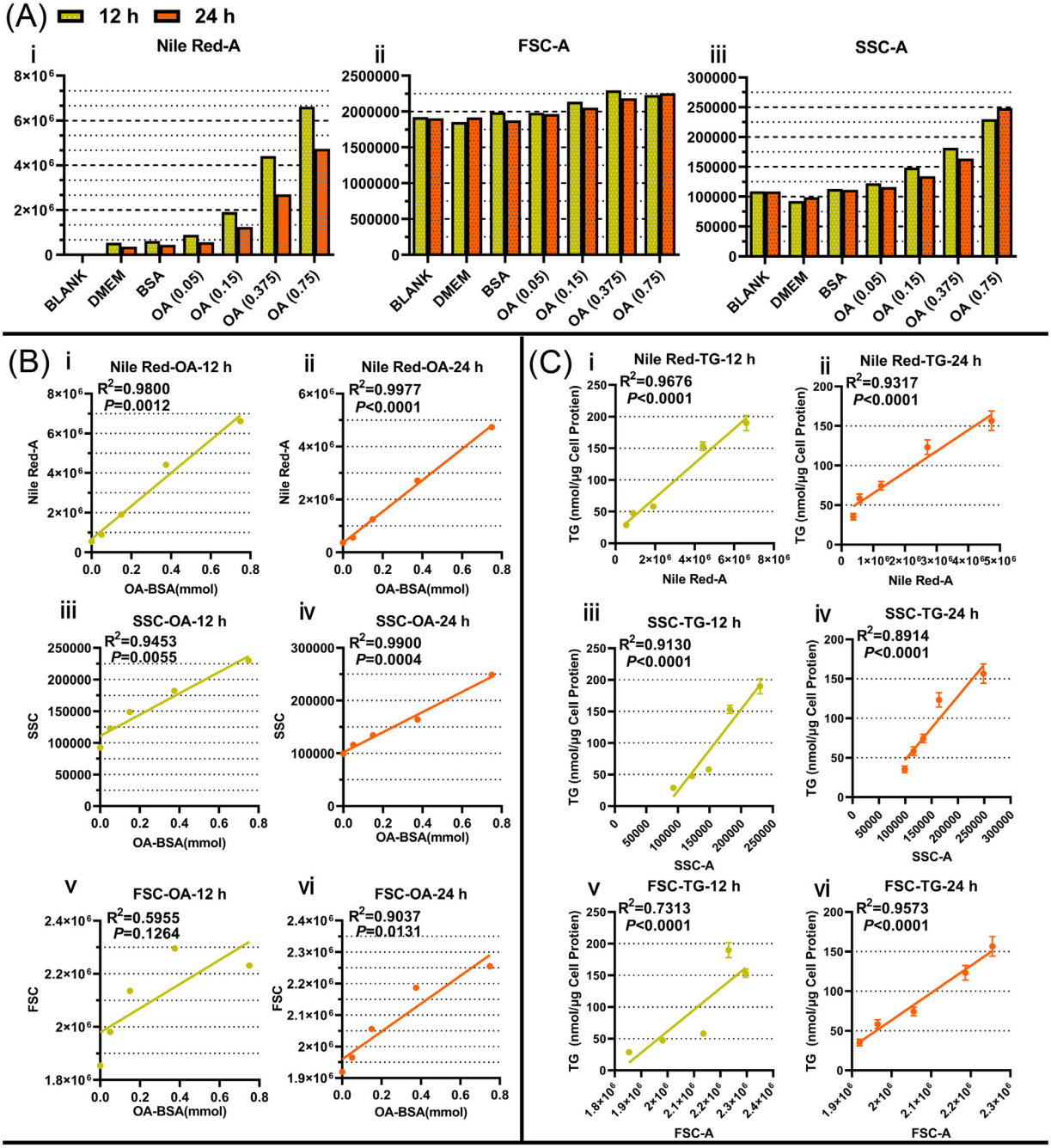

Figure 4. The flow cytometry data were analyzed statistically. Flow cytometry data are summarized in graphs and bar charts generated by GraphPad Prism (A). In particular, our modeling indicates a linear relationship between NileRed-A/FSC-A/SSC-A and OA concentration (B), or between NileRed-A/FSC-A/ SSC-A and TG concentration (C).

examine the effect of OA on lipid metabolism, we tested the expression of LXR or PPAR-γ downstream target genes, such as SREBP-1C/ FASN and MTTP. By regulating the genes for fatty acid synthesis, sterol regulatory element-binding proteins-1 C (**SREBP-1c**, hepatic major isoform of SREBP1) govern overall lipid synthesis in hepatocytes. This study shows that 0.375 and 0.75 mmol/L OA-treatment led to a significant reduction of precursor SREBP-1C (**pSREBP-1C**) and active SREBP-1C (mSREBP-1C) levels in the LMH cells, and that this reduction depends on the increase in the inducing concentration of OA. However, when the concentration of OA was $\leq$0.15 mmol/L, genistein had little impact on pSREBP-1C and mSREBP-1C. Fatty acid synthase (**FASN**) is the rate-limiting enzyme for fatty acid synthesis. We further performed the FASN-target gene analysis, in which expression decreased to significantly lower levels. Statistical analysis of the data showed that FASN down-regulated more than 50% when the OA concentration was higher than 0.15 mmol/L. MTTP is mainly used as a carrier in the endoplasmic reticulum to bind to lipoproteins such as ApoB and is transported out of the liver in the form of VLDL, which plays a critical role in

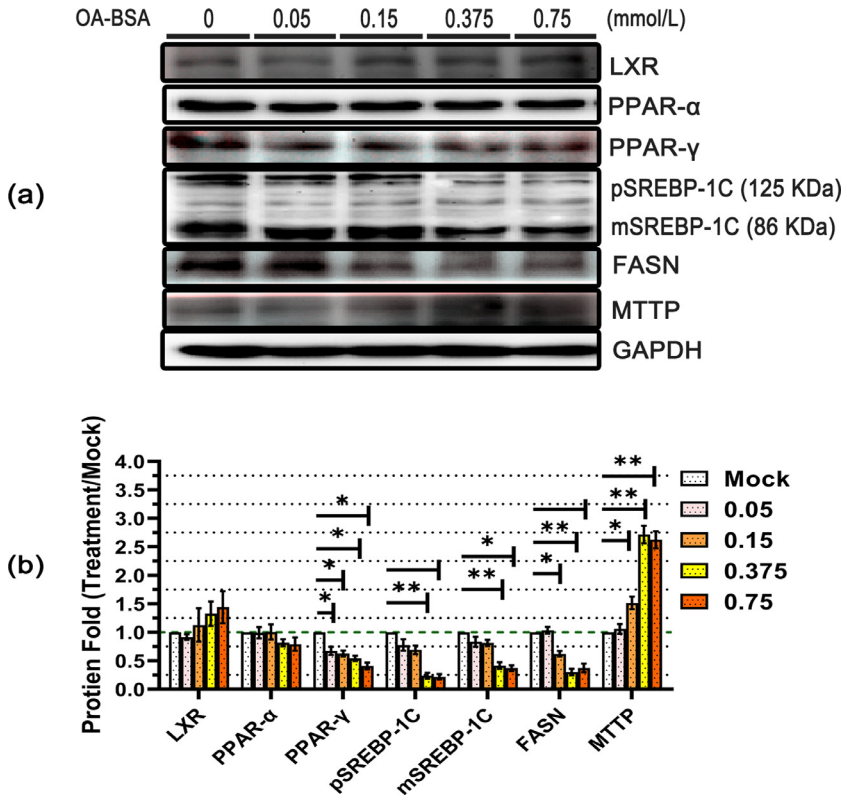

Figure 5. Effects of OA incubated with LMH on fat metabolic pathway-related proteins. The LMH cells were treated with different concentrations of OA (0.05−0.75 mmol/L; n = 3 per group) for 12 h to induce hepatic steatosis, and cells treated with 5% BSA were used as the control. The protein expression of various lipid metabolism-related genes was evaluated by western blot analysis (A). The data were analyzed by ImageJ software to quantify the fluorescence emission from each band, and the relative band intensity was normalized to the mock band. The results of the three independent experiments above were statistically significant and were analyzed by Student's t-test statistical analysis (B). ($P < 0.05$ *, $P < 0.01$ **, $P < 0.001$ ***, $P < 0.0001$ ****).

the assembly and secretion of ApoB-containing lipoproteins. The MTTP levels significantly decreased when the treatment concentration of OA ≥ 0.15 mmol/L in the LMH cells.

The Changes in the Transcript Levels of Genes Involved in fat Metabolism for the Steatosis Model

Next, quantitative PCR (**qPCR**) was performed to test the mRNA expression of key factors for fat metabolism. As shown in Figure 6, the transcription of LXR was not significantly altered in the established steatosis model by OA. In the PPAR family, PPAR-γ mRNA expression was observed to decrease at 12 h and disappeared thereafter. Unlike PPAR-γ, PPAR-α expression was not compromised in those treatments. The mRNA of SREBP-1C was significantly reduced, which was unaffected by the processing time. The transcript levels of the fatty acid synthesis genes, FASN and ACC1, decreased by approximately 2-fold at both time points. In contrast, for the TG synthesis-associated genes, GPAT/PGK1/ACS, the transcript level enhancement was significantly affected by OA at 12 h and completely disappeared at 24 h. HTGL and CPT1A are enzymes related to lipolysis; their expression rapidly increased in LMH cells after OA incubation. HTGL showed the most obvious fold change with a peak of about 10-fold at 24 h. Transcription of FAT (CD36) and L-FABP was enhanced in OA-treated cells, particularly evident at 24 h of treatment. MTTP and ApoB, which play a key role in regulating the secretion of LDL-TG, were significantly increased by OA. Next, we examined the expression of the genes involved in cholesterol metabolism to evaluate the effects of OA on cholesterol metabolism. ABCA1 regulates cholesterol efflux, HMGR is the rate-limiting protein in the cholesterol biosynthetic pathway, L-BABP is an intracellular bile acid transporter in the liver, and QPCR shows those genes with significantly elevated transcription levels treated with OA. This implies that the metabolism of cholesterol was increased by OA treatment in LMH cells.

DISCUSSION

Currently, researchers have established the $HepG_2$ hepatoma cells, L02 human hepatocytes, and Chang liver cells as the models of hepatocyte steatosis for humans. However, for avians, as they differ dramatically from mammals, there is no relevant research on their hepatocyte steatosis model. For this reason, we used the LMH cells to establish a model for avian

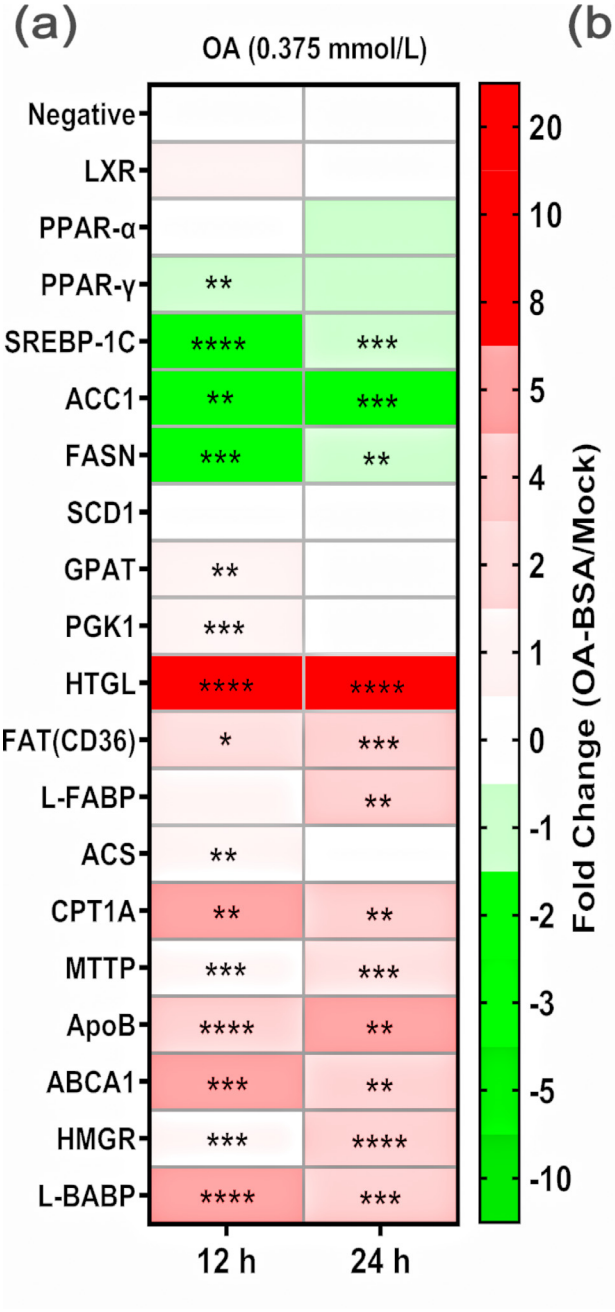

(b)

GENE-Incubation times	Fold Change of mRNA	*P* value
LXR-12 h	1.377	0.013289
LXR-24 h	1.177	0.232259
PPAR-α-12 h	0.982	0.696336
PPAR-α-24 h	0.837	0.116911
PPAR-γ-12 h	0.710	0.005330
PPAR-γ-24 h	0.824	0.143353
SREBP-1C-12 h	0.539	0.000001
SREBP-1C-24 h	0.619	0.000407
ACC1-12 h	0.488	0.008933
ACC1-24 h	0.319	0.000506
FASN-12 h	0.557	0.000258
FASN-24 h	0.647	0.003790
SCD1-12 h	1.287	0.145870
SCD1-24 h	1.105	0.463870
GPAT1-12 h	1.462	0.006559
GPAT1-24 h	0.971	0.615109
PGK1-12 h	1.438	0.000248
PGK1-24 h	0.867	0.144976
HTGL-12 h	5.325	0.000001
HTGL-24 h	10.200	0.000001
FAT(CD36)-12 h	2.106	0.018643
FAT(CD36)-24 h	2.863	0.000220
L-FABP-12 h	1.498	0.122475
L-FABP-24 h	2.982	0.001011
ACS-12 h	1.444	0.003315
ACS-24 h	1.051	0.921187
CPT1A-12 h	4.411	0.007436
CPT1A-24 h	2.109	0.009040
MTP-12 h	1.503	0.000664
MTP-24 h	1.898	0.000148
ApoB-12 h	2.491	0.000002
ApoB-24 h	3.504	0.002015
ABCA1-12 h	3.530	0.000290
ABCA1-24 h	2.051	0.001251
HMGR-12 h	1.413	0.000244
HMGR-24 h	2.508	0.000002
L-BABP-12 h	4.610	0.000005
L-BABP-24 h	2.180	0.000408

Figure 6. Oleic acid was evaluated for the transcription level of fat and cholesterol metabolic pathways on the hepatic steatosis model. LMH cells were treated as described in Figure 5. Total RNA was prepared for transcripts by reverse-transcriptase polymerase chain reaction, and quantitative PCR was performed to characterize fat and cholesterol metabolic pathway gene expression. $P < 0.05$ *, $P < 0.01$ **, $P < 0.001$ ***, $P < 0.0001$ **** (n = 10) vs. control. Abbreviations: ABCA1, ATP-binding cassette transporterA1; Acetyl-CoA Carboxylase-1; ACS, acyl-CoA synthetase; ApoB, Apolipoprotein B; CPT1A, Carnitine O-Palmitoyl transferase 1; FAT/CD36,fatty acid translocase; FASN, fatty acid synthase; GPAT, Glycerol-3-phosphate acyltransferase; HMGR, 3-hydroxy-3-methyl glutaryl coenzyme A reductase; LXR, Liver X Receptor; MTTP, microsomal triglyceride transfer protein; GPADH, Glyceraldehyde-3-phosphate dehydrogenase; PPAR-α, peroxisome proliferator-activated receptor-alpha; PPAR-γ, peroxisome proliferator-activated receptor-gamma; p-ACC, Phospho-Acetyl-CoA Carboxylase; SREBP-1c,sterol regulatory element-binding protein-1c; SCD1, stearoyl−coenzyme A desaturase-1; ACC1, L-BABP, liver bile acid-binding protein; L-FABP, liver-type fatty acid-binding protein; PGK1, Phosphoglycerate kinase 1; SPF Chicken, Specific Pathogen Free chicken.

hepatocyte steatosis due to their immortal characteristics. First, they had the advantages of proliferating rapidly and having a steady-state during culture compared to primary cells. Beyond that, the quality and stability of the LMH cells are aimed at guaranteeing the repeatability of hepatocyte steatosis and future experiments. Therefore, the LMH cells were used to develop and detect the hepatic steatosis model for the study of avian hepatocyte fatty acid metabolism in vitro.

OA is a monounsaturated fatty acid mainly found in vegetable oil. Many studies have shown that hepatocytes uptake OA, esterify it into neutral fat droplets, and stored them. Therefore, researchers use cell OA treatment to establish experimental steatosis models in different types of hepatocytes (HepG2, L02, and Chang

liver cells) (Okamoto et al., 2002; Yanet al., 2015; Hu et al., 2019). In our experiment, similar to most hepatoma cell lines, the LMH cells developed steatosis after treatment with OA. Moreover, we also found that LMH cells treated with 0 to 0.75 mmol/L OA showed dose-dependent lipid accumulation in this study (Figure 1C), which is consistent with the study on a steatosis model in $HepG_2$ by Alkhatatbeh (Alkhatatbeh et al., 2016). Therefore the steatosis models with 0 to 0.75 mmol/L OA, an appropriate dosage regimen for OA treatment, can be formulated based on a linear fit of a TG-OA relation, which provides a feasible approach for the precise regulation of the steatosis hepatocyte model.

Intracellular TGs and lipid droplets are important indicators of the degree of liver steatosis. In this study, the optimal concentration of OA and time of treatment were determined by the results of the CCK assay, NileRed staining, flow cytometry, and TG detection. The results indicated that the number of lipid droplets (Figure 2), the content of triglycerides (Figure 1), and fluorescence intensity (Figure 3B) were significantly higher in the 12 h-treatment group than in 24 h-treatment group after treatment with fixed concentrations of OA, without affecting the viability of the cells. According to the above results, the optimal method for steatosis model establishment was induced by 0.375 mmol/L OA-0.05% BSA for 12 h in LMH cells. In most research dealing with the steatotic hepatocyte model, the cells were treated with different concentrations of OA (<1 mmol/L) and required 24 to 72 h for model establishment (Okamoto et al., 2002; Park et al., 2015; Yan et al., 2015; Hu et al., 2019). The reduction of the time required for steatosis model establishment in the present study was significant compared with that required for the establishment of the other steatosis hepatocyte models ($HepG_2$, L02, etc.). Because of the limited cell life span for each cell generation, the rapid method in this study (12 h) saves more time for the follow-up studies compared to other methods for the establishment of the steatosis models (24−72 h).

A flow cytometry study was performed to support and extend the data obtained by confocal microscopy (Figure 3). We found that, compared to the 0.375 mmol/L OA, LMH showed a significant increase in cellular debris (proportion increased by 43%) but not for the steatosis (proportion increased by 2%) when treated with 0.75 mmol/L OA (Figure 3A). This demonstrates that a higher concentration of OA (greater than or equal to 0.75 mmol/L) increases the degree of cell injury and markedly reduces the intrinsic stability of cells. Furthermore, we observed a highly significant linear relation between NileRed-A and TG concentration (Figure 4C), which shows that NileRed-A fluorescence intensity can reflect the degree of hepatocyte steatosis and thus is a means of steatosis detection. Analysis of FSC and SSC data showed that the size (FSC-A) and granularity (SSC-A) of LMH cells represent an increase in OA-induced steatosis, while only the granularity (SSC-A) is linearly proportional to the OA-induced concentration or the intracellular TG content (Figure 4). It was also found that the intrinsic stability of cells and the degree of steatosis decreased over the OA-induction time at the same concentration in LMH cells. These experimental results support the choice of the optimal inducing concentration, 0.375 mmol/L OA for 12 h.

The presence of OA disturbed the balance between synthesis and consumption, which results in the rapid accrual of glycerolipids, primarily triglycerides, when the LMH steatosis model is being established. To further understand this steatosis model, we conducted several experiments to detect the changes in the intracellular fat metabolism pathway. In the detected nuclear receptor, only the protein and mRNA levels of PPAR-γ were significantly decreased after OA treatment for 12 h. The transcriptional or protein data of lipid metabolism showed that the reactions of fatty acid synthesis (SREBP-1C, ACC1, FASN) were significantly decreased in the LMH steatosis model; the data are consistent with prior studies in $HepG_2$ (Zhang et al., 2019). In our steatosis model, OA also led to significant enhancement of intracellular triglyceride synthesis (GPAT, PGK1), oxidative decomposition of fat (HTGL, ACS, CPT1A), and assembly/secretion of LDL (MTTP, ApoB). Through the comprehensive analysis of the data referred to above, we can presume that OA served as fatty acids to replace the endogenous fatty acids and synthesize triglycerides, which caused a decrease in endogenous fatty acid synthesis and increased intracellular triglyceride synthesis. Apart from this, although the triglyceride decomposition and secretion increased after 12 or 24 h of treatment with OA, this did not have an impact on the rapid accumulation of triglycerides and lipid droplets. The hepatic steatosis model as a first step in the lipid metabolism-related study usually has follow-up processing; therefore, we detected the fat metabolism pathway in the LMH steatosis model at 24 h, to monitor the pathway change over time. There was the only loss of enhancement of triglyceride synthesis (GPAT, PGK1) at 24 h compared with that at 12 h (Figure 6), which indicates that triglycerides do not accumulate further at 24 h. These results, coupled with the enhancement of triglyceride decomposition and secretion, are maintained, which confirms previous results of TG concentration, NileRed stain, and flow cytometry, that steatosis was attenuated at 24 h compared to 12 h in the LMH steatosis model.

In conclusion, we developed a hepatic steatosis model in LMH cells and detected the degree of steatosis by flow cytometry, and also identified the change in the intracellular fat metabolism pathway (Figure 7). This study established an efficient in vitro model for poultry hepatic-related research, which is the first reported steatosis hepatocyte model of poultry and provides valuable clues for investigating the functional mechanisms of poultry liver physiology and pathology in the future.

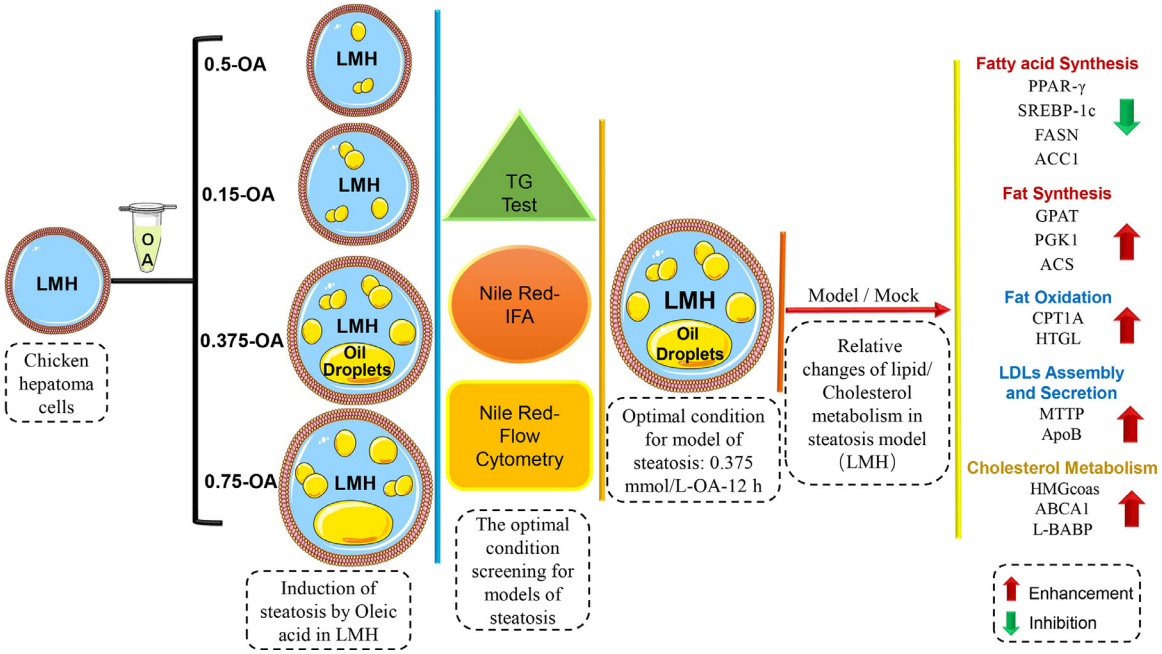

Figure 7. Schematic diagram of the establishment of a steatosis model and changes in its lipid/sterol metabolic pathway.

ACKNOWLEDGMENTS

This research was supported by Postgraduate Research and Innovation Program of Tarim University (TDBSCX202107), China.

DISCLOSURES

We declare that we have no financial and personal relationships with other people or organizations that can inappropriately influence our work, there is no professional or other personal interest of any nature or kind in any product, service and/or company that could be construed as influencing the position presented in, or the review of, the manuscript entitled, "Oleic acid-induced steatosis model establishment in LMH cells and its effect on lipid metabolism".

REFERENCES

Alkhatatbeh, M. J., L. F. Lincz, R. F. Thorne, M. J. Alkhatatbeh, L. F. Lincz, and R. F. Thorne. 2016. Low simvastatin concentrations reduce oleic acid-induced steatosis in HepG2 cells: an invitro model of non-alcoholic fatty liver disease. Exp. Therapeutic Med. 11:1487–1492.

Browning, J. D., L. S. Szczepaniak, R. Dobbins, P. Nuremberg, J. D. Horton, J. C. Cohen, S. M. Grundy, and H. H. Hobbs. 2004. Prevalence of hepatic steatosis in an urban population in the United States: impact of ethnicity. Hepatology 40:1387–1395.

Febbraio, M., S. Reibe, S. Shalapour, G. Ooi, M. Watt, and M. Karin. 2019. Preclinical models for studying NASH-Driven HCC: how useful are they? Cell Metab. 29:18–26.

Feldstein, A. E., N. W. Werneburg, A. Canbay, M. E. Guicciardi, S. F. Bronk, R. Rydzewski, L. J. Burgart, and G. J. Gores. 2004. Free fatty acids promote hepatic lipotoxicity by stimulating TNF-α expression via a lysosomal pathway. Hepatology 40:185–194.

Haghighi-Rad, F., and D. Polin. 1981. The relationship of plasma estradiol and progesterone levels to the fatty liver hemorrhagic syndrome in laying hens. Poult. Sci. 60:2278–2283.

Hu, J., W. Hong, K. Yao, X. Zhu, Z. Chen, and L. Ye. 2019. Ursodeoxycholic acid ameliorates hepatic lipid metabolism in LO2 cells by regulating the AKT/mTOR/SREBP-1 signaling pathway. World J. Gastroenterol. 25:1492–1501.

Lau, J., X. Zhang, and J. Yu. 2017. Animal models of non-alcoholic fatty liver disease: current perspectives and recent advances. J. Pathol. 241:36–44.

Liang, M., Z. Wang, L. Xu, L. Leng, S. Wang, P. Luan, Z. Cao, Y. Li, and H. Li. 2015. Estimating the genetic parameters for liver fat traits in broiler lines divergently selected for abdominal fat. Genet. Mol. Res. 14:9646–9654.

Liu, Z., Q. Li, R. Liu, G. Zhao, Y. Zhang, M. Zheng, H. Cui, P. Li, X. Cui, J. Liu, and J. Wen. 2016. Expression and methylation of microsomal triglyceride transfer protein and acetyl-CoA carboxylase are associated with fatty liver syndrome in chicken. Poult. Sci. 95:1387–1395.

Marchesini, G., M. Brizi, G. Bianchi, S. Tomassetti, E. Bugianesi, M. Lenzi, A. J. McCullough, S. Natale, G. Forlani, and N. Melchionda. 2001. Nonalcoholic fatty liver disease: a feature of the metabolic syndrome. Diabetes 50:1844–1850.

Masahide, H., K. Takao, T. Noriyuki, N. Takayuki, T. Hiroya, F. Kota, O. Tatsushi, N. Tomoaki, S. Hiroshi, S. Makoto, K. Takahiro, O. Junichi, and I. Kazunori. 2005. The metabolic syndrome as a predictor of nonalcoholic fatty liver disease. Ann. Intern. Med. 143:380.

Matteoni, C. A., Z. M. Younossi, T. Gramlich, N. Boparai, Y. C. Liu, and A. J. McCullough. 1999. Nonalcoholic fatty liver disease: a spectrum of clinical and pathological severity. Gastroenterology 116:1413–1419.

Meng, J., N. Ma, H. Liu, J. Liu, J. Liu, J. Wang, X. He, and X. Zhao. 2021. Untargeted and targeted metabolomics profiling reveals the underlying pathogenesis and abnormal arachidonic acid metabolism in laying hens with fatty liver hemorrhagic syndrome. Poult. Sci. 100:101320.

Neuschwander-Tetri. 2001. Non-alcoholic fatty liver disease. BMC Med. 50:1844–1850.

Okamoto, Y., S. Tanaka, and Y. Haga. 2002. Enhanced GLUT2 gene expression in an oleic acid-induced in vitro fatty liver model. Hepatol. Res. 23:138–144.

Park, J.-Y., Y. Kim, J. A. Im, and H. Lee. 2015. Oligonol suppresses lipid accumulation and improves insulin resistance in a palmitate-induced in HepG2 hepatocytes as a cellular steatosis model. BMC Complement Altern. Med. 15:185.

Shini, S., A. Shini, and W. Bryden. 2020. Unraveling fatty liver haemorrhagic syndrome: 1. Oestrogen and inflammation. Avian Pathol. 49:87–98.

Tan, X., R. Liu, S. Xing, Y. Zhang, Q. Li, M. Zheng, G. Zhao, and J. Wen. 2020. Genome-wide detection of key genes and epigenetic markers for chicken fatty liver. Int. J. Mol. Sci. 21:1800.

Tan, X., R. Liu, Y. Zhang, X. Wang, J. Wang, H. Wang, G. Zhao, M. Zheng, and J. Wen. 2021. Integrated analysis of the methylome and transcriptome of chickens with fatty liver hemorrhagic syndrome. BMC Genomics 22:8.

Yan, D., Q. L. Dou, Z. Wang, and Y. Y. W. 2015. Establishment of a hepatocyte steatosis model using Chang liver cells. Genet. Mol. Res. 14:15224–15232.

Yuan, F., L. Hou, L. Wei, R. Quan, J. Wang, H. Liu, and J. Liu. 2021. Fowl adenovirus serotype 4 induces hepatic steatosis via activation of liver X receptor-α. J. Virol. 95:e01938 -01920.

Zhang, J., S. Zhang, P. Wang, N. Guo, W. Wang, L. Yao, Q. Yang, T. Efferth, J. Jiao, and Y. Fu. 2019. Pinolenic acid ameliorates oleic acid-induced lipogenesis and oxidative stress via AMPK/SIRT1 signaling pathway in HepG2 cells. Eur. J. Pharmacol. 861:172618.